Biochemical Pharmacology 80 (2010) 22–30

Contents lists available at ScienceDirect

Biochemical Pharmacology

journal homepage: www.elsevier.com/locate/biochempharm

Dihydroartemisinin accelerates c-MYC oncoprotein degradation and induces apoptosis in c-MYC-overexpressing tumor cells

Jin-Jian Lu [a], Ling-Hua Meng [a,*], Uma T. Shankavaram [b], Cai-Hua Zhu [a], Lin-Jiang Tong [a], Guang Chen [a], Li-Ping Lin [a], John N. Weinstein [c], Jian Ding [a,*]

[a] Division of Anti-tumor Pharmacology, State Key Laboratory of Drug Research, Shanghai Institute of Materia Medica, Chinese Academy of Sciences, 555 Zu Chong Zhi Rd., Shanghai 201203, PR China
[b] Radiation Oncology Branch, National Cancer Institute, NIH, Bethesda, MD, USA
[c] Department of Bioinformatics and Computational Biology, M.D. Anderson Cancer Center, Houston, TX, USA

ARTICLE INFO

Article history:
Received 18 December 2009
Accepted 24 February 2010

Keywords:
Dihydroartemisinin
NCI-60
c-MYC
Apoptosis
GSK 3β

ABSTRACT

Artemisinin and its derivatives (ARTs) are effective antimalarial drugs and also possess profound anticancer activity. However, the mechanism accounted for its distinctive activity in tumor cells remains unelucidated. We computed Pair wise Pearson correlation coefficients to identify genes that show significant correlation with ARTs activity in NCI-55 cell lines using data obtained from studies with HG-U133A Affymetrix chip. We found *c-myc* is one of the genes that showed the highest positive correlation coefficients among the probe sets analyzed ($r = 0.585$, $P < 0.001$). Dihydroartemisinin (DHA), the main active metabolite of ARTs, induced significant apoptosis in HL-60 and HCT116 cells that express high levels of c-MYC. Stable knockdown of *c-myc* abrogated DHA-induced apoptosis in HCT116 cells. Conversely, forced expression of *c-myc* in NIH3T3 cells sensitized these cells to DHA-induced apoptosis. Interestingly, DHA irreversibly down-regulated the protein level of c-MYC in DHA-sensitive HCT116 cells, which is consistent to persistent G1 phase arrest induced by DHA. Further studies demonstrated that DHA accelerated the degradation of c-MYC protein and this process was blocked by pretreatment with the proteasome inhibitor MG-132 or GSK 3β inhibitor LiCl in HCT116 cells. Taken together, ARTs might be useful in the treatment of c-MYC-overexpressing tumors. We also suggest that c-MYC may potentially be a biomarker candidate for prediction of the antitumor efficacies of ARTs.

1. Introduction

Artemisinin, the active principle of Chinese medicinal herb *Artemisia annua* L. (qinghao), and its derivatives (ARTs) are at present widely used as antimalarial drugs without obvious side effects [1,2]. Recently, ARTs have also been studied as candidates for cancer therapy due to their potent antiproliferative activity in various tumor cell lines [3–7]. The further investigation in nude mice bearing human xenograft tumors has demonstrated ARTs could retard the growth of Kaposi's sarcoma, colorectal carcinoma and hepatoma [8–10]. Interestingly, ARTs are active against 55 cell lines of Developmental Therapeutics Program of the U.S. NCI with a unique COMPARE pattern of antiproliferative activity against these cell lines [4,11,12]. That is, ARTs show a COMPARE pattern unlike any other known classes of antitumor agents, suggesting a novel mechanism of action, transport or metabolism. It is believed that the endoperoxide bridge contained in ARTs is required for their activity and ARTs exert the cytotoxic effect by iron-mediated cleavage of the endoperoxide bridge, resulting in induction of toxic free radicals [13,14]. ARTs have been reported to exert their anticancer activity by inducing apoptosis [7,15,16], arresting cells in G1 phase [3,9,15] and antagonizing angiogenesis [10,17,18], etc. However, the mechanism contributed to its distinctive activity in NCI-55 cell lines remains unelucidated.

The oncogene *c-myc* is among the most widely overexpressing oncogenes in human cancers. *c-myc* encodes the c-MYC transcription factor that regulates the expression of diversified target genes, which play important roles in cell proliferation, growth and transformation. Deregulated c-MYC has been shown to increase genomic instability, promote angiogenesis as well as block differentiation [19,20]. Moreover, deregulation of c-MYC has been detected in wide range of human tumors including breast cancer,

Abbreviations: Act D, actinomycin D; ART, artesunate; ARTs, artemisinin and its derivatives; CHX, cycloheximide; DFO, deferoxamine mesylate salt; DHA, dihydroartemisinin; GSK 3β, glycogen-synthase kinase 3β; MB, MYC box; MTT, tetrazolium bromide; NOC, nocodazole; 4-OHT, 4-hydroxy-tamoxifen; PI, propidium iodide; shRNA, short hairpin RNA; SRB, sulforhodamin B; TERT, telomerase reverse transcriptase.

* Corresponding author. Tel.: +86 21 50806722; fax: +86 21 50806722.
E-mail addresses: lhmeng@mail.shcnc.ac.cn (L.-H. Meng), jding@mail.shcnc.ac.cn (J. Ding).

0006-2952/$ – see front matter © 2010 Elsevier Inc. All rights reserved.
doi:10.1016/j.bcp.2010.02.016

colon cancer, melanoma and myeloid leukemia [21,22]. Inactivation of c-MYC resulted in tumor regression accompanied with apoptosis, differentiation or tumor dormancy depending on cell types [23].

In an effort to understand the distinctive activity of ARTs, we studied the correlation between artesunate activity and gene expression in NCI-55 cell lines. *c-myc* is one of the genes showing the highest positive correlation coefficient with an *r* value of 0.585. We found that dihydroartemisinin (DHA), the main active metabolite of ARTs, significantly induced apoptosis in cells which overexpress c-MYC. Down-regulation of *c-myc* by stable transfection of shRNA targeting *c-myc* reduced DHA-induced apoptosis in HCT116 cells. Conversely, forced expression of *c-myc* in NIH3T3 cells sensitized these cells to DHA-induced apoptosis. Furthermore, DHA selectively induced degradation of c-MYC in a proteasome-dependent way in tumor cells overexpressing c-MYC and this process was associated with GSK 3β-mediated phosphorylation of c-MYC at T58 in HCT116 cells.

2. Materials and methods

2.1. Materials

DHA, cycloheximide (CHX), 4-hydroxy-tamoxifen (4-OHT), MG-132, nocodazole (NOC), propidium iodide (PI), sulforhodamine B (SRB) and tetrazolium bromide (MTT) were obtained from Sigma Chemical Co. (St. Louis, MO). Actinomycin D (Act D) was purchased from Amresco (Solon, Ohio). Artesunate was kindly provided by Prof. Ying Li (Shanghai Institute of *Materia Medica*, Shanghai, China).

2.2. Cell lines and culture

The human promyelocytic leukemia HL-60, colorectal carcinoma HCT116, lung adenocarcinoma A549, breast carcinoma MDA-MB-231 and mouse embryonic fibroblast NIH3T3 cell lines were purchased from ATCC (Manassas, VA). HL-60, HCT116, A549, MDA-MB-231 and NIH3T3 cells were maintained in RPMI-1640 (GIBCO, Grand Island, NJ), McCoy's 5A (Sigma), Ham's F12K (GIBCO), Leibovitz's L-15 (GIBCO) and Dulbecco's Modified Eagle Medium (GIBCO), respectively. All of these media were supplemented with 10% heat-inactivated fetal bovine serum (GIBCO), L-glutamine (2 mM), penicillin (100 IU/ml), streptomycin (100 μg/ml) and HEPES (10 mM, pH 7.4). Cells were incubated in a humidified atmosphere of 95% air plus 5% CO_2 at 37 °C.

2.3. Retrovirus production and infection

Phoenix 293 cells obtained from ATCC (Manassas, VA) were transfected with the retroviral vectors pBabe-puro-myc.ER or pRetrosuper myc shRNA using Lipofectamine 2000 (Invitrogen). pBabe-puro-myc.ER was kindly provided by Prof. Steven Mcmahon and Dr. Xiao-Yong Zhang (Thomas Jefferson University) and pRetrosuper myc shRNA was obtained from Addgene (Addgene plasmid 15662, donated by Dr. Martin Eilers) [24]. Forty-eight hours after transfection, retroviral supernatant was collected and filtered through a 0.45-μm filter. Retrovirus supplemented with 5 μg/ml polybrene was used to infect NIH3T3 or HCT116 cells. Antibiotic selection was carried out 48 h later in the presence of 2 μg/ml puromycin for 7 days. The established cell lines were named as NIH3T3/myc.ER and HCT116/shmyc, respectively.

2.4. Establishment of DHA-resistant HCT116 subline

The DHA-resistant HCT116 cell line was established as described previously [25]. HCT116 cells were exposed to 10 μM DHA for 72 h and then were cultured in fresh medium until the surviving cells had recovered and displayed a normal exponentially growing manner. The cycles of selection were performed in the presence of gradually increasing concentrations of DHA from 10 μM to 100 μM. After 45 cycles, the cells were subjected to a one-step selection process in the presence of 200 μM DHA. Surviving colonies were harvested and propagated in drug-free medium for further studies. The newly established DHA-resistant HCT116 subline was designated as HCT116/R. During the establishment of HCT116/R cell line, its parental HCT116 cell line was always maintained in drug-free medium in parallel.

2.5. Statistical methods for analysis of ARTs activity and gene expression data

Gene expression patterns for the NCI-55 cell lines were assessed using data from studies with HG-U133A Affymetrix chip. GI_{50}s of ARTs (artesunate, NSC 712571; artemisinin, NSC 369397; artemether, NSC 665970; arteether, NSC 665971) against the NCI-55 panel was obtained from the Developmental Therapeutics Program screen (http://www.dtp.nci.nih.gov/docs/dtp_search.html) with a selected set of 1429 drugs that had been tested multiple times and whose screening data met previously established quality control criteria [26]. The methodology of statistical analyses has previously been described in detail [27,28].

2.6. Cell proliferation assays

The antiproliferative activity of ARTs was determined by MTT assay in suspended cells (HL-60) or SRB assay in adherent cells (HCT116, A549 and MDA-MB-231) as described before [29]. Inhibitory rate of the cell proliferation was calculated as: $[1 - (A_{570\ \text{treated}}/A_{570\ \text{control}})] \times 100\%$ (MTT assay) or $[1 - (A_{515\ \text{treated}}/A_{515\ \text{control}})] \times 100\%$ (SRB assay).

2.7. Flow cytometry analysis of DNA content

Cells seeded in 6-well plates were treated with DHA for indicated time. Cells were harvested and fixed in 70% ethanol and then stored at 4 °C overnight. Cells were stained in PBS containing 40 μg/ml RNase and 10 μg/ml PI in dark at room temperature for 30 min and analyzed using an FACS-Calibur cytometer (Becton Dickinson, San Jose, CA). At least 10,000 events were counted for each sample.

2.8. Annexin V-FITC assay

Cells seeded in 6-well plates were exposed to DHA at a range of concentrations for indicated times. Cells undergoing apoptosis were detected using an Annexin V-FITC apoptosis detection kit (KeyGEN, Nanjing, China). Briefly, cells were resuspended in cold binding buffer and incubated for 15 min in the dark at room temperature following addition of 5 μl of Annexin V-FITC and 5 μl of PI solutions. Flow cytometry analysis was performed using an FACS-Calibur cytometer (Becton Dickinson, San Jose, CA).

2.9. Real-time PCR

HCT116 cells were treated with 10 μM DHA for indicated times and total RNA was extracted using Trizol (Invitrogen) according to the manufacturer's protocol. The primer sequences were as follows: 5′-CTGGTGCTCCATGAGGAG-3′ (forward) and 5′-AGGTGATCCAGACTCTGAC-3′ (reverse) for *c-myc*; 5′-CCATGGAGAAGGCTGGGG-3′ (forward); and 5′-CAAATGTGTCATGGATGACC-3′ (reverse) for *GAPDH*. One microgram of total RNA was reversely transcribed using the PrimeScript™ RT reagent kit (TaKaRa, Dalian, China) and the cDNA template was amplified by real-time PCR

using the SYBR® *Premix EX Taq*™ II kit (TaKaRa, Dalian, China). Thermal cycling was programmed as follows: 95 °C for 30 sec followed by 35 cycles of 95 °C for 5 s, 64 °C for 20 s and 72 °C for 15 s, and then 72 °C for 10 min. Gene expression was assessed by delta C_t method and mRNA levels of *c-myc* were normalized to those of *GAPDH* internal standard.

2.10. Western blot analysis

Western blot analyses for c-MYC, phosphorylated c-MYC and telomerase reverse transcriptase (TERT) were conducted as previously described [30], with the antibodies against c-MYC (#9402), phosphorylated c-MYC (#9401) (Cell Signaling Technology, Beverly, MA); TERT (NB 600-476, NOVUS Biologicals, Littleton, CO) and GAPDH (KC-5G4, KangChen Biotechnology, Shanghai, China).

2.11. Statistical analysis

Data were presented as mean ± SD from at least three separate experiments, and significance was analyzed with Student's *t*-test. Differences were considered significant where $P < 0.05$.

3. Results

3.1. c-MYC expression is highly correlated with ARTs antiproliferative activity

Among the four ARTs (artesunate, NSC 712571; artemisinin, NSC 369397; artemether, NSC 665970; arteether, NSC 665971) screened by NCI Developmental Therapeutics Program, artesunate (NSC 712571) displays most potent activity in NCI-55 cell

(A)

Rank	Gene name	Gene description	*r*	*P*-value
1	*SFRS2*	splicing factor, arginine/serine-rich 2	0.599	<0.001
2	*MRPL16*	mitochondrial ribosomal protein L16	0.595	<0.001
3	*CABC1*	chaperone, ABC1 activity of bc1 complex homolog (S. pombe)	0.594	<0.001
4	*MYC*	v-myc myelocytomatosis viral oncogene homolog (avian)	0.585	<0.001
5	*C15orf15*	chromosome 15 open reading frame 15	0.582	<0.001
6	*PTMA*	prothymosin, alpha	0.578	<0.001
7	*EIF4B*	eukaryotic translation initiation factor 4B	0.577	<0.001
8	*LETMD1*	LETM1 domain containing 1	0.574	<0.001
9	*MAX*	MYC associated factor X	0.572	<0.001
10	*ARHGAP4*	Rho GTPase activating protein 4	0.571	<0.001

(B)

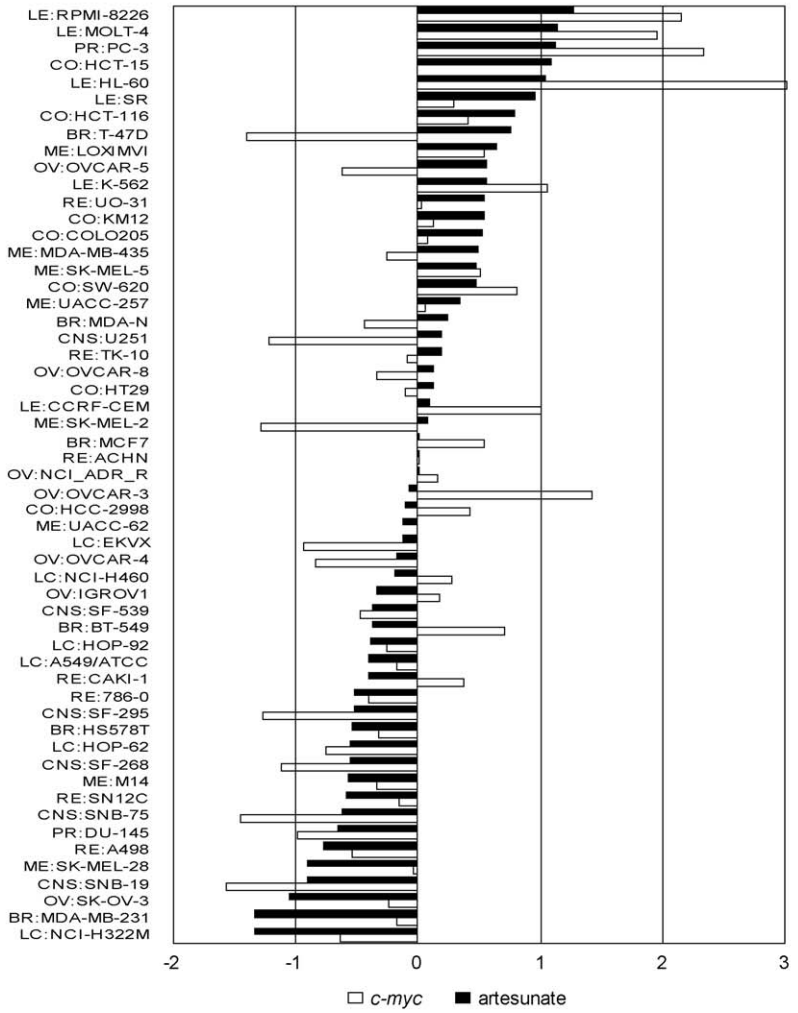

Fig. 1. (A) Pearson correlation (*r*) between the antiproliferative activity of artesunate ($-\log_{10} GI_{50}$) and gene expression patterns in the NCI-55 cell lines based on data from the Affymetrix HG-U133A chip. Genes presented were first ten genes that are most positively correlated in order of their *P*-values. *P*-values were calculated by multivariate permutation test as described previously [27]. (B) Relative artesunate activity (solid box) and *c-myc* expression (hollow box) in NCI-55 cell lines were listed by artesunate activity.

lines. To understand the unique antiproliferative activity pattern of artesunate in the NCI-55 cell line screen, we computed pairwise Pearson correlation coefficients (r) between the activity of artesunate and gene expression levels for each cell line. Even though similar analysis has been performed by Efferth et al. [4], where 170 genes were included for correlative analysis, we expanded this analysis to 12,000 probe sets. Genes presented in Fig. 1A are first 10 genes that are most positively correlated to the antiproliferative activity of artesunate. The oncogene *c-myc* was found to be one of the most highly positively correlated genes with an r value of 0.585. *c-myc* has been shown to be positively correlated with the anticancer activity of artesunate with an r value of 0.38498 [4]. The difference between the r values may be due to different number of genes tested. Nevertheless, both studies found *c-myc* expression positively correlated with artesunate activity. We also preformed same analysis in the activities of artemisinin, artemether and arteether and found *c-myc* consistently appeared as one of the most correlated genes ($P < 0.001$) (data not shown). Interestingly, the c-MYC cofactor MAX is also among the first ten highly positively correlated genes. We thus chose *c-myc* for further study and plotted *c-myc* expression levels and artesunate activity in the NCI-55 cell lines (Fig. 1B). The activity of artesunate and expression of *c-myc* tend in the same direction, indicating positive correlation: the higher the *c-myc* expression, the greater the sensitivity of a given cell line. However, it should be noted that *c-myc* expression does not correlate well with artesunate activity in all the cell lines tested. For example, some cell lines, such as OVCAR-3 and CCRF-CEM, were relatively resistant to DHA even though their *c-myc* levels are high. Overall, these data suggest the importance of *c-myc* expression for artesunate activity against at least some of the cell types.

To further test the positive correlation between c-MYC expression and ARTs activity, we detected c-MYC expression in HL-60, HCT-116, A549 and MDA-MB-231 cells according to their sensitivities to artesunate presented in Fig. 1B. HL-60 and HCT116 cells express relatively high level of c-MYC, whereas A549 and MDA-MB-231 cells express much lower level of c-MYC (Fig. 2A), which is consistent with the microarray analysis. The antiproliferative activity of artesunate in these four cell lines was further evaluated and found that HCT116 and HL-60 cells were more sensitive to artesunate than A549 and MDA-MB-231 cells, confirming the positive correlation between c-MYC expression and artesunate activity (Fig. 2B, top). Because DHA is the major active metabolite of ARTs, we measured the antiproliferative activity of DHA in these four cell lines and obtained similar antiproliferative pattern in cell lines tested (Fig. 2B, bottom). We further detected DHA-induced apoptosis by evaluating Annexin V-positive cells in these four cell lines. Because HL-60 cells are rather sensitive to DHA-induced apoptosis ([7], Fig. 2B), they were treated with DHA at lower concentration for a relative shorter time compared with other cells. As shown in Fig. 2C, HL-60 and HCT116 cells were more sensitive than A549 and MDA-MB-231 cell to DHA-induced apoptosis, indicating DHA activity is also highly correlated to c-MYC expression. Therefore, DHA was utilized in the following experiments.

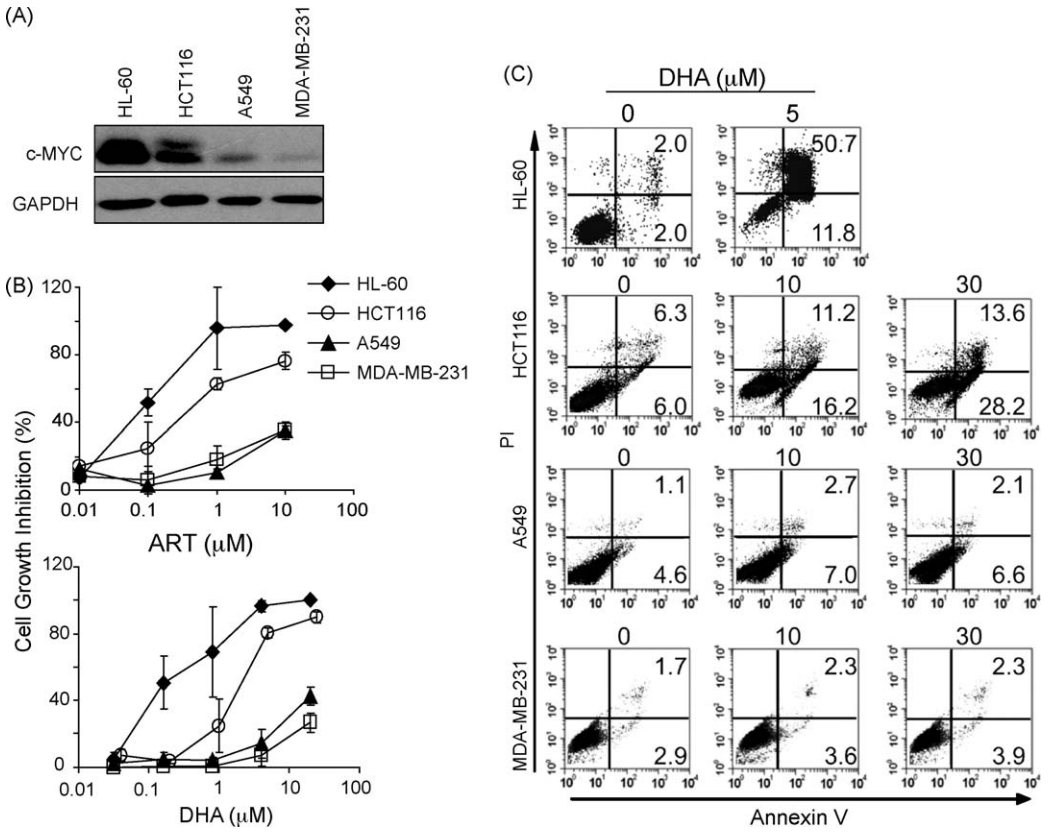

Fig. 2. Tumor cells expressing different levels of c-MYC displays distinct sensitivity in DHA-induced inhibition of cell proliferation and apoptosis. (A) The protein levels of c-MYC in HL-60, HCT116, A549 and MDA-MB-231 cells were detected by Western blot. (B) Antiproliferative activity was assessed by MTT assay (HL-60) or SRB (HCT116, A549 and MDA-MB-231) assay after continuous exposure to artesunate (ART, top panel) or DHA (lower panel) for 72 h. Data show were mean ± SD of three independent experiments. (C) DHA displays different activity in inducing apoptosis in HL-60, HCT116, A549 and MDA-MB-231 cells. Cells were treated with DHA for 24 h (HL-60) or 48 h (HCT116, A549 and MDA-MB-231) and the apoptotic cells were determined by Annexin V-PI double staining followed by flow cytometric analysis. Cell in the upper right quadrants (Annexin V^+/PI^+) were recognized as late apoptotic cells and those in the lower right quadrants (Annexin V^+/PI^-) were calculated as cells undergoing early apoptosis. Data shown in each quadrant represented the percentage of cells tested in each example and are representative of at least two independent experiments.

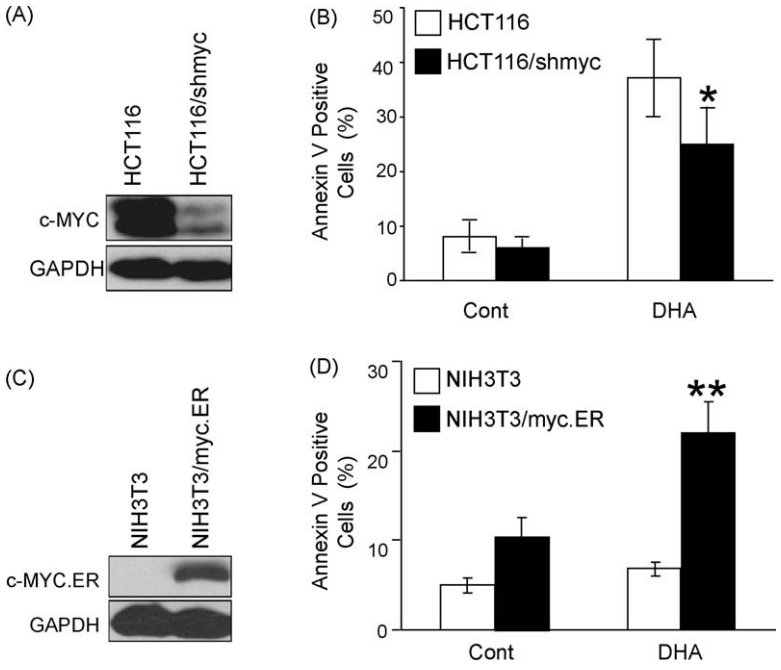

Fig. 3. Genetically modifications of *c-myc* expression profoundly influence the activity of DHA-induced apoptosis. (A) The protein levels of c-MYC in HCT116 and HCT116/shmyc cells were detected by Western blot. (B) Induction of apoptosis by DHA in HCT116 and HCT116/shmyc cells. Cells were treated with 30 μM DHA for 48 h and the apoptotic cells were measured by Annexin V-PI staining and flow cytometry. The data were presented as mean ± SD, $n = 3$. $^{*}P < 0.05$. HCT116/shmyc cells treated with DHA compared with HCT116 cells with the same treatment. (C) The protein levels of c-MYC.ER in NIH3T3 and NIH3T3/myc.ER cells. (D) Induction of apoptosis by DHA in NIH3T3 and NIH3T3/myc.ER cells. Cells were pretreated with 100 nM 4-OHT and then concurrently treated with 30 μM DHA for 24 h. Apoptotic cells were detected by Annexin V-PI staining and flow cytometry. The data were expressed as mean ± SD, $n = 3$. $^{**}P < 0.01$. NIH3T3/myc.ER cells treated with DHA compared with NIH3T3 cells with the same treatment.

3.2. Knocking down c-myc reduces induction of apoptosis by DHA

To investigate whether knocking down *c-myc* in DHA-sensitive cells would influence the ability of DHA to induce apoptosis, a cell line named HCT116/shmyc was established, in which c-MYC expression was significantly down-regulated by stable expression of shRNA targeting *c-myc* (Fig. 3A). HCT116/shmyc and the parent HCT116 cells were treated with indicated concentrations of DHA for 48 h and the apoptotic cells were detected using Annexin V-PI staining. As shown in Fig. 3B, there were nearly 40% of HCT116 cells undergoing apoptosis after treatment 30 μM DHA. By contrast, there were 25% apoptotic cells in HCT116/shmyc cells upon the same treatment, indicating down-regulation of c-MYC renders HCT116 cells resistant to DHA-induced apoptosis.

3.3. Transfection with c-myc renders NIH3T3 cells sensitive to DHA

To determine whether cells with enhanced expression of *c-myc* could gain sensitivity to DHA, we ectopically overexpressed *c-myc* in NIH3T3 cells by introducing a chimeric protein c-MYC.ER (Fig. 3C), which consists of human *c-myc* fused at its carboxyl terminus to the hormone-binding domain of a mutant mouse estrogen receptor [31]. In the presence of 4-OHT, the c-MYC.ER protein translocates to the nuclear and is activated as a transcription factor. Pretreatment of NIH3T3/myc.ER cells with 100 nM 4-OHT for 24 h partially reversed G1/S arrest induced by serum deprivation (data not shown), indicating that c-MYC.ER fusion protein functioned properly to promote progression of cell cycle. NIH3T3/myc.ER cells were then treated with DHA for 48 h and apoptosis was detected by Annexin V-PI double staining. As shown in Fig. 3D, less than 10% of NIH3T3 cells were Annexin V-positive with or without DHA treatment. However, 20% of NIH3T3/myc.ER cells were Annexin V-positive after treatment with 30 μM DHA, indicating forced expression of *c-myc* sensitize NIH3T3 cell to DHA-induced apoptosis. This data together with the results presented in Fig. 3B confirm the positive correlation between the anticancer activity of DHA and c-MYC expression.

3.4. DHA reduces the protein level and disrupts the function of c-MYC in HCT116 cells

To investigate whether DHA has any effect on the expression of c-MYC, HCT116 cells were treated with various concentrations of DHA for indicated times. As shown in Fig. 4A, c-MYC protein showed a slight decrease at 6 h and declined significantly after treatment with DHA for 12 h. DHA also induced down-regulation of c-MYC in a concentration-dependent manner (Fig. 4A, right panel). We further measured the protein level of TERT, which is expressed under the control of c-MYC [32]. As shown in Fig. 4B, DHA treatment caused decrease in TERT, confirming that DHA decreases c-MYC expression and further leads to compromise in its function.

To examine whether DHA-induced down-regulation of c-MYC is reversible, HCT116 cell were first treated with 10 μM DHA for 24 h to induce reduction of c-MYC (Fig. 4C, T-24). Cells were further incubated in DHA-free medium for another 24 h. As shown in Fig. 4C, c-MYC remained at low level after removal of DHA for 24 h (R-24), indicating down-regulation of c-MYC by DHA is persistent in the time frame tested. We next examined whether DHA-induced G1 phase arrest is also irreversible. As shown in Fig. 4D, DHA treatment arrested HCT116 cells in G1 phase (T-24). Then DHA was washed out and both DHA-treated or -untreated cells were further incubated in fresh medium containing nocodazole (a mitotic inhibitor agent which exerts its effect by depolymerizing microtubules) for an additional 24 h (R-24). DHA-untreated cells were arrested by nocodazole at M phase (Fig. 4D, R-24). By contrast, DHA-treated cells remained in G1 phase irrespective of presence of nocodazole, demonstrating irreversible G1 phase arrest by DHA. The consistency between c-MYC reduction and G1 phase arrest induced by DHA suggested down-regulation of c-MYC may

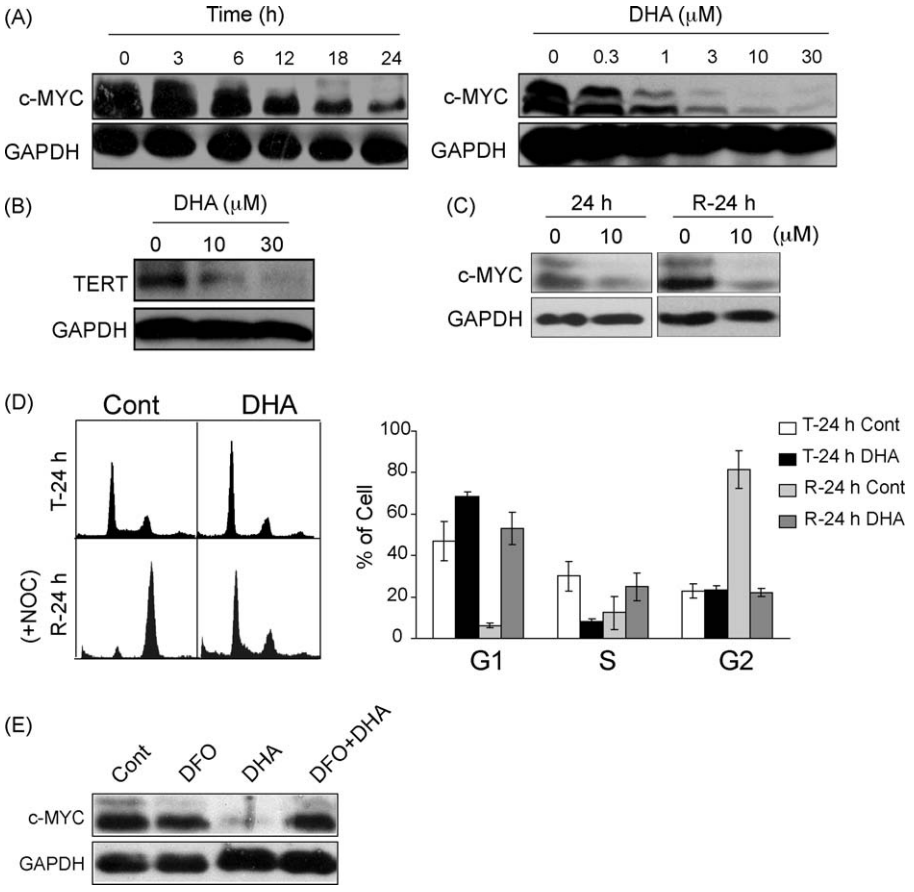

Fig. 4. DHA reduces the protein level and disrupts the function of c-MYC in HCT116 cells. (A) DHA time- and concentration-dependently reduces c-MYC protein in HCT116 cells. Cells were incubated with 10 μM DHA for indicated times (left panel) or different concentrations of DHA for 18 h (right panel). (B) DHA disrupts the function of c-MYC in HCT116 cells. Cells were treated with indicated concentrations of DHA for 24 h and the TERT level was detected using Western blot. (C) DHA-induced down-regulation of c-MYC is irreversible. Cells were first treated with 10 μM DHA for 24 h and further incubated in DHA-free medium for another 24 h. Western blot was performed to detect c-MYC level. (D) DHA irreversible induced HCT116 cells at G1 phase arrest. Cells were first treated with 10 μM DHA for 24 h (T-24 h) and further incubated in DHA-free medium containing 200 ng/ml NOC for additional 24 h (R-24 h). Data shown were percentage of cell population in G1, S or G2 phase. (E) DFO abrogates DHA-induced c-MYC degradation. HCT116 cells were pretreated with 25 μM DFO for 6 h and co-incubated with DHA for another 24 h. Data shown are representative or mean ± SD from at least three independent experiments.

contribute to the cell cycle arrest induced by DHA as this protein is a key molecular for cells progression from G1 to S phase.

It is believed that iron plays vital role in the anticancer activity of ARTs [7,14], we proposed that DHA-induced decrease in c-MYC was also iron-dependent. HCT116 cells were pretreated with the iron chelator DFO and then co-incubated with DHA for 24 h. As shown in Fig. 4E, DFO significantly reversed the down-regulation of c-MYC by DHA, further supporting the notion that down-regulation of c-MYC is associated with its anticancer activity.

3.5. DHA selectively reduces c-MYC protein level in DHA-sensitive tumor cells

To detect whether DHA-induced down-regulation of c-MYC is a universal phenomenon in tumor cells, HL-60, A549 and MDA-MB-231 cells were treated with various concentrations of DHA for 24 h and c-MYC level was examined by Western blot assay. c-MYC protein remarkably decreased in DHA-sensitive HL-60 cells but not in A549 and MDA-MB-231 cells upon DHA treatment (Fig. 5A). In order to further illuminate this question, we established a DHA-resistant HCT116 subline named HCT116/R which was resistant to DHA-induced apoptosis (Fig. 5B). Interestingly, this cell line expressed relatively low c-MYC protein compared with the parental HCT116 cells and DHA had little effect on the c-MYC protein level in this cell line (Fig. 5C). All these data demonstrate that DHA reduces c-MYC only in DHA-sensitive cells. This notion together with the fact that c-MYC depletion precedes DHA-induced apoptosis suggested that down-regulation of c-MYC might be important for DHA-induced apoptosis.

3.6. DHA accelerated degradation of c-MYC in a proteasome-dependent way

To dissect the detailed mechanism of the c-MYC reduction imposed by DHA, the mRNA level of *c-myc* were first measured by real-time PCR in HCT116 cells treated with DHA. As shown in Fig. 6A, DHA treatment had little effect on the mRNA level of *c-myc* in the pharmacological concentration range. As expected, the mRNA level of *c-myc* decreased significantly in the presence of the RNA synthesis inhibitor Act D, which was included as a positive control.

Because unchanged mRNA level of *c-myc* could not explain down-regulation of protein level upon DHA treatment. We determined the degradation kinetics of c-MYC after DHA treatment. In this assay, HCT116 cells were first treated with 10 μM DHA for 18 h, and then concurrently with CHX for different times (Fig. 6B). Cells were then collected to examine the protein level of c-MYC (Fig. 6C). The half life of c-MYC protein was about 40 min in untreated HCT116 cells (Fig. 6C and D). DHA treatment accelerated the degradation of c-MYC with a shorter half life of 20 min (Fig. 6C and D), indicating that down-regulation of c-MYC by DHA is due to enhanced degradation.

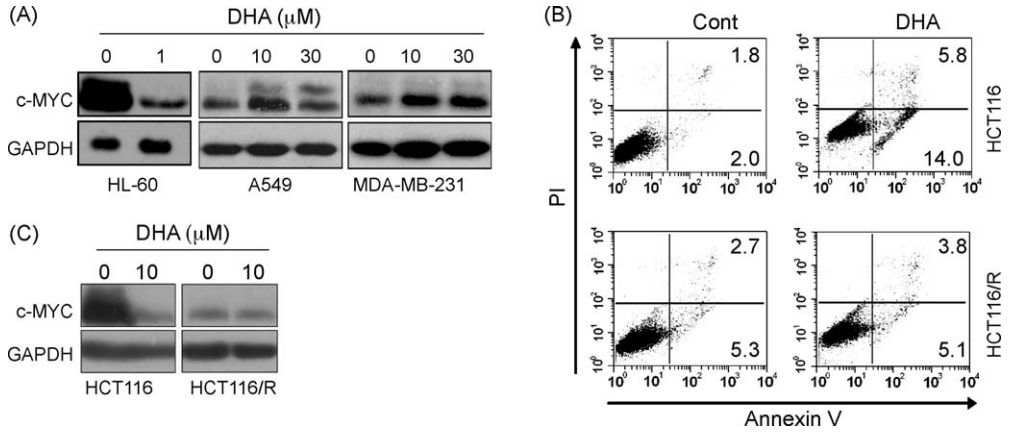

Fig. 5. DHA selectively reduces the protein level of c-MYC in DHA-sensitive tumor cells. (A) DHA reduces c-MYC protein in HL-60 cells but not in A549 and MDA-MB-231 cells. Cells were treated with indicated concentrations of DHA for 24 h and the protein level of c-MYC was detected by Western blot. (B) HCT116/R cells are resistant to DHA-induced apoptosis. HCT116/R cells resistant to DHA were established as described in Materials and methods. Cells were treated with 10 μM DHA for 48 h and the apoptotic cells were examined by Annexin V-PI double staining and flow cytometry. The percentage of Annexin V-positive cells in the top (PI positive) and bottom (PI negative) right quadrants was indicated. (C) DHA-resistant HCT116/R cells express low level of c-MYC. The levels of c-MYC were detected after cells were incubated with 10 μM DHA for 24 h. Data shown are representative for at least three independent experiments.

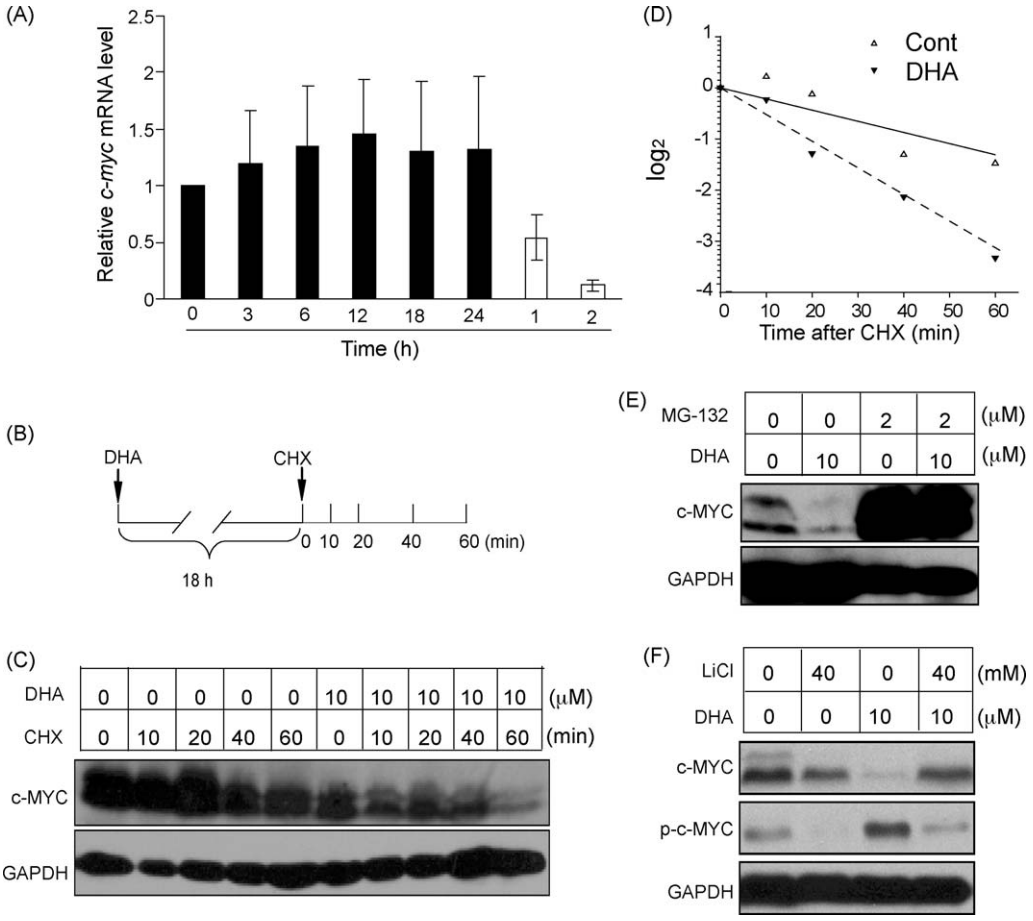

Fig. 6. Enhanced degradation of c-MYC by DHA in a proteasome-dependent pathway is associated with GSK 3β. (A) DHA does not affect *c-myc* mRNA level in HCT116 cells. HCT116 cells were treated with 10 μM DHA for indicated times and the mRNA level was determined by real-time PCR. 5 μg/ml Act D was used as a positive control (white bar). (B) A schematic representation of the experimental protocol. HCT116 cells were exposed to 10 μM DHA for 18 h, then concurrently with CHX (100 ng/ml) for indicated times. (C) c-MYC levels were determined by Western blot. This figure was representative for at least three experiments. GAPDH was used as a loading control. (D) Quantitation of protein degradation kinetics from three representative independent experiments. c-MYC band intensities were normalized to those of GAPDH, then normalized to the t_0 controls. Each decrease of one unit of $\log_2$ (band intensity) was equivalent to one half-life. (E) MG-132 abrogates DHA-induced c-MYC protein depletion in HCT116 cells. HCT116 cells were pretreated with 2 μM MG-132 for 1 h, and then co-exposed to 10 μM DHA for 18 h. Data shown were representative for three independent experiments. (F) GSK 3β inhibitor LiCl blocks DHA-induced c-MYC protein degradation in HCT116 cells. HCT116 cells were pretreated with 40 mM LiCl for 1 h, and then co-exposed to 10 μM DHA for 24 h. Data shown were representative for three independent experiments.

The stability of c-MYC protein is regulated through mechanisms that ultimately control ubiquitin-mediated degradation by the 26S proteasome [33]. We proposed that DHA-induced destabilization of c-MYC might result from increased proteasomal degradation. To test this hypothesis, HCT116 cells were treated with DHA in the presence of proteasome inhibitor MG-132. Blocking proteasome function prevented the decrease of c-MYC (Fig. 6E), suggesting that DHA depletes c-MYC level through a proteasome-dependent degradation process in HCT116 cells. Furthermore, MG-132 also abrogated DHA-induced downregulation of c-MYC level in HL-60 cells (data not shown). However, distinct from in HCT116 cells, *c-myc* gene is amplified in HL-60 cells. We could not exclude other mechanisms may also involved in the reduction of c-MYC by DHA in HL-60 cells, which deserves further study. Nevertheless, our present data indicated that accelerated degradation of c-MYC at least partially responsible for DHA-induced reduction of c-MYC in HL-60 cells.

3.7. DHA accelerates c-MYC degradation via enhanced T58 phosphorylation in HCT116 cells

Because phosphorylation of c-MYC at T58 promotes its degradation [34–36], it is possible that DHA-induced c-MYC depletion is due to phosphorylation of c-MYC at T58. To test this possibility, phosphorylated c-MYC were detected after DHA treatment using antibody selectively recognizing c-MYC phosphorylated at T58/S62. As shown in Fig. 6F, while the whole protein level of c-MYC decreased, phosphorylated c-MYC increased. Because phosphorylation at Ser 62 stabilizes c-MYC [37], c-MYC detected by the phosphorylated-specific antibody used should bear phosphorylation at T58. It has been demonstrated that glycogen-synthase kinase 3β (GSK 3β) phosphorylated c-MYC at T58 and triggered its proteasomal degradation in response to stimuli [38]. To examine whether GSK 3β is involved in the increased phosphorylated c-MYC at T58 in response to DHA, HCT116 cells were pretreated with GSK 3β inhibitor LiCl before DHA addition. LiCl prevented the phosphorylation of c-MYC and abrogated DHA-induced c-MYC degradation (Fig. 6F). Thus, increased phosphorylation of c-MYC at T58 is coincided with its proteasome-dependent degradation induced by DHA.

4. Discussion

ARTs have been demonstrated to exert their anticancer activity in an iron-dependent way and to induce cell cycle arrest or apoptosis in various tumor cell types [7,9,14–16]. In this study, we correlated ARTs activity profile (GI_{50}s) with gene expression in the NCI-55 cell lines and found that the oncogene *c-myc* is among the genes showing the highest positive correlation coefficients. Genetically regulation of *c-myc* expression profoundly influenced the activity of DHA to induce apoptosis. We further demonstrated that DHA remarkably enhanced phosphorylation of c-MYC and accelerated degradation of c-MYC protein via the proteasome pathway. These results help to shed a new light into mechanism of action of DHA.

The MYC family includes c-MYC, N-MYC and L-MYC. Among them, c-MYC shows the most frequency of aberrations [19]. This oncogene is activated in 20% of all human cancers [21,39]. Overexpression of *c-myc* was found in 67% colon cancers and even 91% in Burkitt's lymphoma [40,41]. Deregulated MYC expression leads to dependency of developing cancer cells to the resulting aberrant MYC functions, referred as "oncogene addiction". Herein, we found that *c-myc* is one of the most highly correlated genes with the anticancer activity of ARTs. We further tested this correlation in four cell lines originated from different tissue types. HCT116 and HL-60 cells that overexpress c-MYC were sensitive to ARTs-induced proliferation inhibition and apoptosis. By contrast, A549 and MDA-MB-231 cells that express low levels of c-MYC were resistant to ARTs. These results confirmed the positive correlation between c-MYC expression and the anticancer activity of ARTs. Moreover, the newly-established DHA-resistant HCT116/R cell line also expressed much less c-MYC compared with the parent HCT116 cells though the mechanisms are still unclear. This notion was further supported by the observations obtained from cells with genetic modification of *c-myc*: stable knockdown of *c-myc* using shRNA reduced DHA-induced apoptosis in HCT116 cells, while forced expression of *c-myc* in NIH3T3 cells sensitized these cells to DHA-induced apoptosis. The selectivity of ARTs against c-MYC-overexpressing tumors cells provides a rationale for potential use of ARTs in the treatment c-MYC-overexpressing tumors, which also indicates its safety to the majority of normal cells that express low levels of c-MYC.

Of particular note, DHA was found to significantly reduce the level of c-MYC protein. Recent study demonstrated that brief inactivation of MYC leads to induction of apoptosis in tumors and subsequent tumor regression [23]. Many strategies are under development to target c-MYC [19,42], such as disrupting c-MYC expression by targeting cascades ranging from transcription to translation (antisense oligonucleotides, small interfering RNA, tetraplex forming oligonucleotides, decoy oligonucleotides and so on) or alternatively blocking its function by inhibiting critical protein-protein interactions [43,44]. In this study, we found that DHA reduced c-MYC protein level in HCT116 cells by accelerating the degradation of c-MYC and resulted in disruption of its function. On the contrary, DHA had marginal effect on the expression of *c-myc* at mRNA level at the pharmacological concentrations (Fig. 6). Protein is the presenter of function after all and depletion of c-MYC also disrupts the interaction between c-MYC and its partner proteins, therefore degradation of c-MYC may be more efficient compared with other strategies. DHA-induced specific degradation of c-MYC also partially explained its selectivity against c-MYC-overexpressing tumor cells. Moreover, degradation of c-MYC disrupted its function as well as the addiction of tumor cells to c-MYC and resulted in cell cycle arrest and apoptosis. This notion was also supported by the fact that DHA-induced irreversible down-regulation of c-MYC was accompanied with irreversible G1 phase arrest. Finally, it is also noteworthy that DFO co-treatment abrogated DHA-induced c-MYC degradation, indicating iron-mediated activation of DHA is required for c-MYC degradation. This further demonstrates the important role of iron in ARTs anticancer activity.

The stability of c-MYC is generally regulated through ubiquitin-mediated degradation by the 26S proteasome [33]. Consistently, we found proteasome inhibitor MG-132 abrogated DHA-induced degradation of c-MYC. The NH_2-terminal region of c-MYC contains two highly conserved sequences known as MYC box I (MB I) and MB II, which play vital roles in regulating the stability of c-MYC. The phosphorylation pattern at T58 and S62 within MB I determines c-MYC stability [37], while the MBII together with the COOH-terminal domain are necessary for c-MYC degradation under some specific conditions [45,46]. In most cases, c-MYC that is targeted for degradation by the proteasome pathway is marked by GSK 3β-mediated phosphorylation at T58 [36]. In this study, we also demonstrated that DHA-induced degradation of c-MYC in HCT116 cells was associated with GSK 3β-mediated phosphorylation of c-MYC at T58. Our unpublished data and other study [47] indicated that ARTs induced endoplasmic reticulum stress, which might result in GSK 3β-mediated signaling [48]. However, further study needs to be performed to elucidate how GSK 3β is activated upon the treatment of DHA.

In summary, we found ARTs induced rapid degradation of c-MYC and preferentially inhibition proliferation in tumor cells

overexpressing c-MYC. The positive correlation between c-MYC expression and ARTs anticancer activity, together with the fact that ARTs induced degradation of c-MYC provide rationale that ARTs might be useful in the treatment of c-MYC overexpressing tumors. We also suggest that c-MYC could potentially be developed into a biomarker candidate for prediction of the antitumor efficacies of ARTs at least in some tumor types.

Acknowledgements

This work was supported by the National Natural Science of China (nos. 30701026 and 30721005), National Science & Technology Major Project "Key New Drug Creation and Manufacturing Program" (2009ZX09301-001). We thank Dr. Qin Chen and Dr. Zhi-Xiang Zhang for their help in the real-time PCR assay. We also thank Dr. Yi Jiang for his help in establishing DHA resistant HCT116/R cell line.

References

[1] Woerdenbag HJ, Pras N, van Uden W, Wallaart TE, Beekman AC, Lugt CB. Progress in the research of artemisinin-related antimalarials: an update. Pharm World Sci 1994;16:169–80.
[2] O'Neill PM, Posner GH. A medicinal chemistry perspective on artemisinin and related endoperoxides. J Med Chem 2004;47:2945–64.
[3] Li Y, Wu JM, Shan F, Wu GS, Ding J, Xiao D, et al. Synthesis and cytotoxicity of dihydroartemisinin ethers containing cyanoarylmethyl group. Bioorg Med Chem 2003;11:977–84.
[4] Efferth T, Sauerbrey A, Olbrich A, Gebhart E, Rauch P, Weber HO, et al. Molecular modes of action of artesunate in tumor cell lines. Mol Pharmacol 2003;64:382–94.
[5] Efferth T, Olbrich A, Bauer R. mRNA expression profiles for the response of human tumor cell lines to the antimalarial drugs artesunate, arteether, and artemether. Biochem Pharmacol 2002;64:617–23.
[6] Disbrow GL, Baege AC, Kierpiec KA, Yuan H, Centeno JA, Thibodeaux CA, et al. Dihydroartemisinin is cytotoxic to papillomavirus-expressing epithelial cells in vitro and in vivo. Cancer Res 2005;65:10854–61.
[7] Lu JJ, Meng LH, Cai YJ, Chen Q, Tong LJ, Lin LP, et al. Dihydroartemisinin induces apoptosis in HL-60 leukemia cells dependent of iron and p38 mitogen-activated protein kinase activation but independent of reactive oxygen species. Cancer Biol Ther 2008;7:1017–23.
[8] Li LN, Zhang HD, Yuan SJ, Tian ZY, Wang L, Sun ZX. Artesunate attenuates the growth of human colorectal carcinoma and inhibits hyperactive Wnt/beta-catenin pathway. Int J Cancer 2007;121:1360–5.
[9] Hou J, Wang D, Zhang R, Wang H. Experimental therapy of hepatoma with artemisinin and its derivatives: in vitro and in vivo activity, chemosensitization, and mechanisms of action. Clin Cancer Res 2008;14:5519–30.
[10] Dell'Eva R, Pfeffer U, Vene R, Anfosso L, Forlani A, Albini A, et al. Inhibition of angiogenesis in vivo and growth of Kaposi's sarcoma xenograft tumors by the anti-malarial artesunate. Biochem Pharmacol 2004;68:2359–66.
[11] Efferth T, Dunstan H, Sauerbrey A, Miyachi H, Chitambar CR. The anti-malarial artesunate is also active against cancer. Int J Oncol 2001;18:767–73.
[12] Efferth T. Mechanistic perspectives for 1,2,4-trioxanes in anti-cancer therapy. Drug Resist Updat 2005;8:85–97.
[13] Mercer AE, Maggs JL, Sun XM, Cohen GM, Chadwick J, O'Neill PM, et al. Evidence for the involvement of carbon-centered radicals in the induction of apoptotic cell death by artemisinin compounds. J Biol Chem 2007;282:9372–82.
[14] Efferth T, Benakis A, Romero MR, Tomicic M, Rauh R, Steinbach D, et al. Enhancement of cytotoxicity of artemisinins toward cancer cells by ferrous iron. Free Radic Biol Med 2004;37:998–1009.
[15] Jiao Y, Ge CM, Meng QH, Cao JP, Tong J, Fan SJ. Dihydroartemisinin is an inhibitor of ovarian cancer cell growth. Acta Pharmacol Sin 2007;28:1045–56.
[16] Chen T, Li M, Zhang R, Wang H. Dihydroartemisinin Induces Apoptosis and Sensitizes Human Ovarian Cancer Cells to Carboplatin Therapy. J Cell Mol Med 2009;13:1358–70.
[17] Chen HH, Zhou HJ, Wang WQ, Wu GD. Antimalarial dihydroartemisinin also inhibits angiogenesis. Cancer Chemother Pharmacol 2004;53:423–32.
[18] Lee J, Zhou HJ, Wu XH. Dihydroartemisinin downregulates vascular endothelial growth factor expression and induces apoptosis in chronic myeloid leukemia K562 cells. Cancer Chemother Pharmacol 2006;57:213–20.
[19] Vita M, Henriksson M. The Myc oncoprotein as a therapeutic target for human cancer. Semin Cancer Biol 2006;16:318–30.
[20] Pelengaris S, Khan M, Evan G. c-MYC: more than just a matter of life and death. Nat Rev Cancer 2002;2:764–76.
[21] Dang CV. c-Myc target genes involved in cell growth, apoptosis, and metabolism. Mol Cell Biol 1999;19:1–11.
[22] Schlagbauer-Wadl H, Griffioen M, van Elsas A, Schrier PI, Pustelnik T, Eichler HG, et al. Influence of increased c-Myc expression on the growth characteristics of human melanoma. J Invest Dermatol 1999;112:332–6.
[23] Jain M, Arvanitis C, Chu K, Dewey W, Leonhardt E, Trinh M, et al. Sustained loss of a neoplastic phenotype by brief inactivation of MYC. Science 2002;297:102–4.
[24] Popov N, Wanzel M, Madiredjo M, Zhang D, Beijersbergen R, Bernards R, et al. The ubiquitin-specific protease USP28 is required for MYC stability. Nat Cell Biol 2007;9:765–74.
[25] Miao ZH, Tong LJ, Zhang JS, Han JX, Ding J. Characterization of salvicine-resistant lung adenocarcinoma A549/SAL cell line. Int J Cancer 2004;110:627–32.
[26] Scherf U, Ross DT, Waltham M, Smith LH, Lee JK, Tanabe L, et al. A gene expression database for the molecular pharmacology of cancer. Nat Genet 2000;24:236–44.
[27] Meng LH, Shankavaram U, Chen C, Agama K, Fu HQ, Gonzalez FJ, et al. Activation of aminoflavone (NSC 686288) by a sulfotransferase is required for the antiproliferative effect of the drug and for induction of histone gamma-H2AX. Cancer Res 2006;66:9656–64.
[28] Rao VA, Agama K, Holbeck S, Pommier Y. Batracylin (NSC 320846), a dual inhibitor of DNA topoisomerases I and II induces histone gamma-H2AX as a biomarker of DNA damage. Cancer Res 2007;67:9971–9.
[29] Tao Z, Zhou Y, Lu J, Duan W, Qin Y, He X, et al. Caspase-8 preferentially senses the apoptosis-inducing action of NG-18, a Gambogic acid derivative, in human leukemia HL-60 cells. Cancer Biol Ther 2007;6:691–6.
[30] Xie H, Qin YX, Zhou YL, Tong LJ, Lin LP, Geng MY, et al. GA3, a new gambogic acid derivative, exhibits potent antitumor activities in vitro via apoptosis-involved mechanisms. Acta Pharmacol Sin 2009;30:346–54.
[31] Littlewood TD, Hancock DC, Danielian PS, Parker MG, Evan GI. A modified oestrogen receptor ligand-binding domain as an improved switch for the regulation of heterologous proteins. Nucleic Acids Res 1995;23:1686–90.
[32] Wu KJ, Grandori C, Amacker M, Simon-Vermot N, Polack A, Lingner J, et al. Direct activation of TERT transcription by c-MYC. Nat Genet 1999;21:220–4.
[33] Sears R, Nuckolls F, Haura E, Taya Y, Tamai K, Nevins JR. Multiple Ras-dependent phosphorylation pathways regulate Myc protein stability. Genes Dev 2000;14:2501–14.
[34] Hann SR. Role of post-translational modifications in regulating c-Myc proteolysis, transcriptional activity and biological function. Semin Cancer Biol 2006;16:288–302.
[35] Vervoorts J, Luscher-Firzlaff J, Luscher B. The ins and outs of MYC regulation by posttranslational mechanisms. J Biol Chem 2006;281:34725–9.
[36] Sears RC. The life cycle of C-myc: from synthesis to degradation. Cell Cycle 2004;3:1133–7.
[37] Yeh E, Cunningham M, Arnold H, Chasse D, Monteith T, Ivaldi G, et al. A signalling pathway controlling c-Myc degradation that impacts oncogenic transformation of human cells. Nat Cell Biol 2004;6:308–18.
[38] Gregory MA, Qi Y, Hann SR. Phosphorylation by glycogen synthase kinase-3 controls c-myc proteolysis and subnuclear localization. J Biol Chem 2003;278:51606–12.
[39] Nesbit CE, Tersak JM, Prochownik EV. MYC oncogenes and human neoplastic disease. Oncogene 1999;18:3004–16.
[40] Frost M, Newell J, Lones MA, Tripp SR, Cairo MS, Perkins SL. Comparative immunohistochemical analysis of pediatric Burkitt lymphoma and diffuse large B-cell lymphoma. Am J Clin Pathol 2004;121:384–92.
[41] Smith DR, Myint T, Goh HS. Over-expression of the c-myc proto-oncogene in colorectal carcinoma. Br J Cancer 1993;68:407–13.
[42] Ponzielli R, Katz S, Barsyte-Lovejoy D, Penn LZ. Cancer therapeutics: targeting the dark side of Myc. Eur J Cancer 2005;41:2485–501.
[43] Yin X, Giap C, Lazo JS, Prochownik EV. Low molecular weight inhibitors of Myc-Max interaction and function. Oncogene 2003;22:6151–9.
[44] Berg T, Cohen SB, Desharnais J, Sonderegger C, Maslyar DJ, Goldberg J, et al. Small-molecule antagonists of Myc/Max dimerization inhibit Myc-induced transformation of chicken embryo fibroblasts. Proc Natl Acad Sci USA 2002;99:3830–5.
[45] Kim SY, Herbst A, Tworkowski KA, Salghetti SE, Tansey WP. Skp2 regulates Myc protein stability and activity. Mol Cell 2003;11:1177–88.
[46] von der Lehr N, Johansson S, Wu S, Bahram F, Castell A, Cetinkaya C, et al. The F-box protein Skp2 participates in c-Myc proteosomal degradation and acts as a cofactor for c-Myc-regulated transcription. Mol Cell 2003;11:1189–200.
[47] Stockwin LH, Han B, Yu SX, Hollingshead MG, ElSohly MA, Gul W, et al. Artemisinin dimer anticancer activity correlates with heme-catalyzed reactive oxygen species generation and endoplasmic reticulum stress induction. Int J Cancer 2009;125:1266–75.
[48] Meares GP, Zmijewska AA, Jope RS. HSP105 interacts with GRP78 and GSK3 and promotes ER stress-induced caspase-3 activation. Cell Signal 2008;20:347–58.